Astron. Astrophys. 318, 631–638 (1997)

ASTRONOMY
AND
ASTROPHYSICS

UESAC – The Uppsala-ESO survey of asteroids and comets⋆

O. Hernius[1,5], **C.-I. Lagerkvist**[1,3], **M. Lindgren**[1], **G. Tancredi**[2], **and G. V. Williams**[4]

[1] Astronomiska observatoriet, Box 515, S-752 20 Uppsala, Sweden
[2] Depto. de Astronomia, Facultad de Ciencias, Tristan Narvaja 1674, 11200 Montevideo, Uruguay
[3] Institute for Planetary Exploration DLR, Rudower Chausse 5, D-10489 Berlin, Germany
[4] Minor Planet Center, Smithsonian Astrophysical Observatory, Cambridge, MA 02138, USA
[5] Observatorio, Pl 14, FIN-00014 Helsingin Yliopisto, Finland

Received 3 June 1996 / Accepted 19 August 1996

Abstract. More than 15 000 positions of moving objects have been detected on 74 plates and films obtained at the European Southern Observatory in Chile and the Anglo-Australian Observatory in Australia during Jupiter's oppositions in 1992 and 1993. Two or more positions have been secured for about 3400 asteroids, and orbits have so far been calculated for about 2500 asteroids. The majority of these asteroids are previously undetected.

We present apparent magnitudes for all observed asteroids and absolute magnitudes for those asteroids with orbits. We present model-diameters based on a Monte Carlo approach using the albedo distribution found by the IRAS Minor Planet Survey (Tedesco et al. 1992). Model-diameters are also calculated for the asteroids observed in the Palomar-Leiden Survey of Faint Minor Planets, PLS, (van Houten et al. 1970). Statistics of orbital elements are presented and compared with the results of the PLS.

Key words: minor planets; asteroids – surveys – solar system: general

1. Introduction

The Uppsala-ESO Survey of Asteroids and Comets (hereafter UESAC) was undertaken to search for unknown comets in the neighbourhood of Jupiter (Tancredi and Lindgren 1994; Lindgren et al. 1995). UESAC consists of surveys around the time of Jupiter's opposition in both 1992 and 1993. A total of 74 plates and films were obtained at the European Southern Observatory in Chile (ESO) and the Anglo-Australian Observatory in Australia (AAO). The plates and films were scanned manually and more than 15 000 trails of moving objects were detected and measured.

In Sects. 2, 3 and 4 we present the main details concerning the observations, reductions and linkage of moving objects. A more thorough description can be found in Lagerkvist et al. (1995), hereafter L95. Statistics of apparent and absolute magnitudes are presented in Sect. 4. We present model-diameters for the asteroids observed in UESAC and the Palomar-Leiden Survey of Faint Minor Planets, hereafter PLS (van Houten et al. 1970), in Sect. 5 and statistics of orbital elements are presented in Sect. 6.

2. Observations

The 1992 and 1993 observing campaigns (hereafter UESAC'92 and UESAC'93) were carried out in similar, but not identical, fashions. Each campaign covered a $16^\circ \times 16^\circ$ region, centred on Jupiter. Nine plates, each covering $5\overset{\circ}{.}4 \times 5\overset{\circ}{.}4$, were exposed on each of three nights during one week in March 1992 and March 1993. Follow-up observations were carried out during the next new moon period in April of each year. The centres of the April fields were shifted about 6° to the west of the March fields to compensate for one month's motion of the main-belt objects. The 1992 March and 1993 March plates were exposed for 90 and 105 minutes, respectively. In the 1993 campaign the shutter was closed for 15 minutes after 60 minutes exposure, producing two trails of each object. This approach helped to distinguish between asteroids and stars since the short end of a star trail almost always points in the opposite direction from an asteroid trail. To optimize the limiting magnitude for objects in the neighbourhood of Jupiter, the plates were tracked at the apparent motion of the planet. The April plates and films were tracked at sidereal rate and exposed for 45 minutes. Seeing conditions were considerably better during the 1993 campaign, a fact which is partly reflected in the greater number of asteroids detected in that survey. We have adopted mean seeing disks of $1\overset{''}{.}5$ for 1992 and $1\overset{''}{.}0$ for 1993 (L95). Table 1 gives information on the number of detected trails in each campaign.

Send offprint requests to: C.-I. Lagerkvist

⋆ Based on observations collected at the European Southern Observatory, La Silla, Chile

Table 1. Number of trails detected on the plates and films.

Survey	March plates	April plates/films
1992	4502	774
1993	7922	1904

Table 2. Average quality of the plate reductions.

	$\overline{\sigma_\alpha}$	$\overline{\sigma_\delta}$	N_{REF}
1992 Section 3	$0\farcs814$	$0\farcs770$	72 – 50
1992 Section 2	$0\farcs607$	$0\farcs593$	69 – 37
1992 Section 1	$0\farcs352$	$0\farcs335$	43 – 22
1993 Section 3	$0\farcs956$	$0\farcs832$	38 – 25
1993 Section 2	$0\farcs676$	$0\farcs517$	33 – 19
1993 Section 1	$0\farcs410$	$0\farcs380$	26 – 19

2.1. Plate reductions

The deduced J2000.0 topocentric astrometric positions are based on a reference frame defined by PPM and SAO reference stars (Röser and Bastian 1991). The uncertainties given in Table 2 are standard deviations of the comparison-star residuals (least-squares plate-solution position minus catalogued position). The three different sections refers to three concentric regions on the plates; the reductions were performed separately for each region. The number of included reference stars in the reductions are N_{REF}. A more thorough description of the astrometry may be found in L95.

2.2. Linkage of moving objects

Initial linkage of objects observed on the March plates was performed by extrapolation of the motion vectors derived from the trails. Extension of the linkages to the April objects was more problematic: secure linkage of the March and April objects required observations on pairs of nights in each month. The 1993 campaign was planned with this requirement, but due to a malfunction of the plate vault at ESO, which destroyed most of the unexposed photographic plates, this could not be achieved. As a result, many of the month-to-month linkages were uncertain. Although great caution was exercised in making these linkages, a number have subsequently been shown to be incorrect, through the identification of observations of specific objects at other oppositions. In some cases, confirmation of the UESAC April observations was obtained from observations made by other observers—notably the Spacewatch telescope at Kitt Peak.

Failure to make linkages from March to April was also caused by objects moving out of the field covered in April or by objects being too faint to be observed one month past opposition. Table 3 gives the number of linked UESAC observations. The numbers in the $N \geq 1$ ... $N \geq 5$ columns refers to objects with at least N linked UESAC observations. The numbers in the M-A column refers to observations of objects linked from March to April. The numbers in the $N \geq 1$ column do not include the unlinked April positions. The observations were reported to the Minor Planet Center where they were checked for identifications with known numbered or multiple-opposition unnumbered asteroids, as well as with new one-opposition objects. In addition, observations belonging to the outer Jovian satellites were identified (Hernius et al. 1996). The 2956 unidentified objects that had been observed on more than one night were assigned provisional designations.

Table 3. Number of linked UESAC observations.

Survey	$N \geq 1$	$N \geq 2$	$N \geq 3$	$N \geq 4$	$N \geq 5$	M-A
1992	2559	1176	775	309	30	325
1993	3984	2250	1554	523	66	525

Table 4. Mean apparent magnitude differences (ephemeris minus UESAC) for the numbered asteroids included in the data fit.

Plates	$\overline{\lvert\Delta V\rvert}$	$\overline{\Delta V}$	$\sigma_{\Delta V}$	N_{APP}
March 1992	$0\fm48$	$0\fm00$	$0\fm61$	98
March 1993	$0\fm61$	$0\fm00$	$0\fm77$	104

3. Magnitudes

3.1. Determination and accuracy of apparent magnitudes

A complete description of the apparent magnitude calculation can be found in L95; here we present the main features. The apparent magnitudes were estimated by assigning one of eight brightness classes to each object while performing the astrometric measurements. A linear data fit between the magnitude estimates and the ephemeris V-magnitudes of the observed numbered objects was used to derive magnitudes for all the UESAC objects. This analysis was performed separately for the 1992 and 1993 objects. The magnitudes were corrected for trailing using the trail-correction equation:

$$\Delta m \;=\; -2.5 \log_{10} \frac{l/d}{1.06\; erf(0.83\; l/d)} \qquad (1)$$

(Tancredi and Lindgren 1994) where l is the trail length, d the size of the seeing disk and *erf* the error function.

We define the mean errors for the V-magnitudes as the mean difference between the magnitudes of the numbered asteroids derived from the above analysis and the corresponding ephemeris values. These errors are only valid for $V < 18$, since most of the numbered asteroids included in the fits are brighter than this value. Table 4 gives the mean differences (ephemeris minus UESAC) for the 1992 and 1993 observing campaigns separately. The number of numbered asteroids included in the analysis is N_{APP} and the standard deviations for the errors with regard to sign are also given.

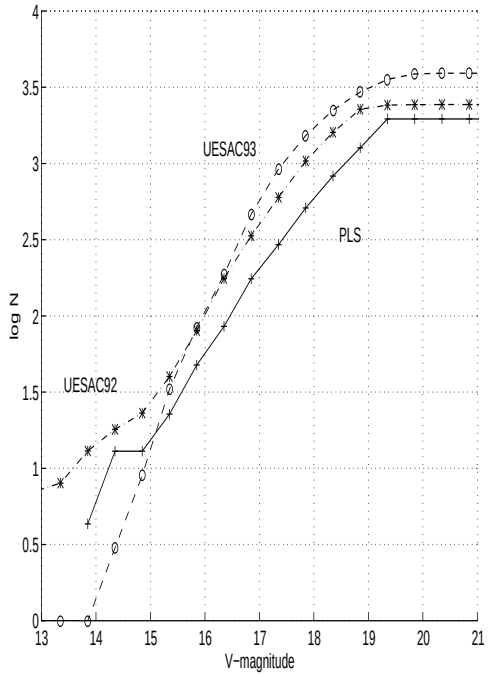

Fig. 1. The logarithm of the cumulative number of asteroids per half-magnitude step for UESAC'92, UESAC'93 and PLS.

3.2. Statistics of apparent magnitudes

The following statistics are based on the UESAC March magnitudes; the magnitudes for the unlinked April positions are not included. A mean magnitude was used for each discrete object, so no asteroid should therefore appear more than once in the statistics. The PLS numbers are based on asteroids with a determined orbit. Since the regions investigated by PLS and UESAC differ both in size and centre coordinates, the PLS numbers (van Houten et al. 1970) have been multiplied by a factor of 1.08 (L95). The PLS m-magnitudes (International Photometric Magnitude System) were transformed to V-magnitudes (L95). Fig. 1 shows the cumulative number of asteroids per half magnitude step, starting from $V = 12.85$, for UESAC'92, UESAC'93 and PLS asteroids. The PLS numbers in the interval $V = [18.85, 19.35]$ were corrected for incompleteness (van Houten et al. 1970). The somewhat peculiar V-magnitude intervals are a result of the fact that the PLS numbers were given as number of asteroids per half m-magnitude. The linear parts of the curves can be represented by expressions of the form:

$$\log N_{1992} = -7.11 + 0.57V \quad (2)$$

$$\log N_{1993} = -8.80 + 0.68V \quad (3)$$

$$\log N_{PLS} = -6.90 + 0.54V \quad (4)$$

The expressions are based on points in the interval $V = [15.35, 17.85]$.

Table 5. Mean absolute magnitude differences (ephemeris minus UESAC) for the observed numbered asteroids

Plates	$\overline{\lvert\Delta H\rvert}$	$\overline{\Delta H}$	$\sigma_{\Delta H}$	$N_{\rm ABS}$
March 1992	$0^m.69$	$+0^m.00$	$0^m.93$	52
March 1993	$0^m.65$	$-0^m.06$	$0^m.88$	81

3.3. Determination and accuracy of absolute magnitudes

The calculation of the absolute magnitudes was done according to the HG-system (Bowell et al. 1989); a thorough description can be found in L95.

We define the mean errors for the absolute magnitudes as the mean differences between the H-magnitudes of the observed numbered asteroids and the corresponding EMP/MPC H-magnitudes (EMP = *Efemeridy Malykh Planet/Ephemerides of Minor Planets*, MPC = *Minor Planet Circulars*). Table 5 gives the mean differences (ephemeris minus UESAC) for the 1992 and 1993 observing campaigns separately. The number of numbered asteroids included in the analysis is N_{ABS} and the standard deviations for the errors with regard to sign are also given. For some numbered asteroids an orbit could not be calculated based on the UESAC observations; these asteroids have therefore been excluded from the error analysis. The errors with regard to sign are not significant.

3.4. Statistics of absolute magnitudes

The statistics in this section are based on H-magnitudes for UESAC and PLS asteroids with determined orbits. Fig. 2 shows the logarithm of the cumulative numbers of absolute magnitudes per 0.25-magnitude step in UESAC'92, UESAC'93 and PLS. The PLS H-magnitudes are taken from EMP/MPC files and not from the values given in van Houten et al. (1970). As a result of differences in the survey coverage the PLS numbers have been multiplied by 0.90 (L95). The linear parts of the curves can be represented by expressions of the form:

$$\log N_{1992} = -3.53 + 0.44H \quad (5)$$

$$\log N_{1993} = -4.25 + 0.52H \quad (6)$$

$$\log N_{PLS} = -4.44 + 0.49H \quad (7)$$

The expressions are based on points in the interval $H = [11.00, 14.00]$.

4. Model diameters

Precise knowledge of the geometric albedo is needed if diameter calculation is to be attempted for individual asteroids. However, if the main goal is to examine the diameter distribution for a set of asteroids, it is possible to make use of the albedo distribution of the numbered asteroids. Previous results (Zellner and Bowell 1977, Ishida et al. 1984 and Gradie and Tedesco 1982) show a decreasing albedo-trend with increasing heliocentric distance.

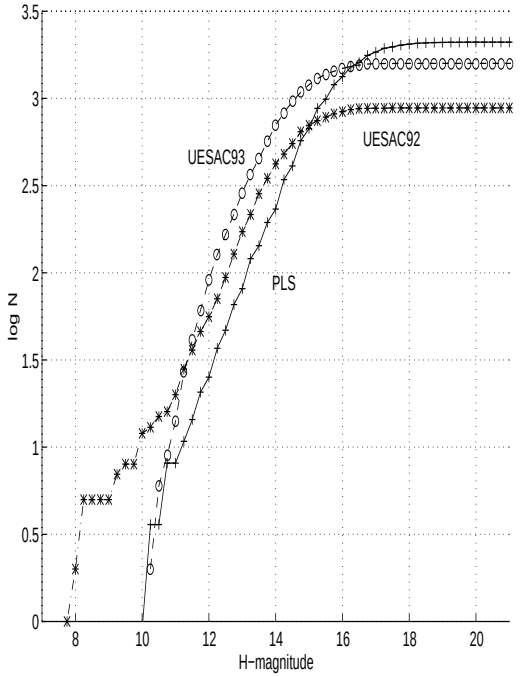

Fig. 2. The logarithm of the cumulative number of asteroids per 0.25 magnitude for UESAC'92, UESAC'93 and PLS.

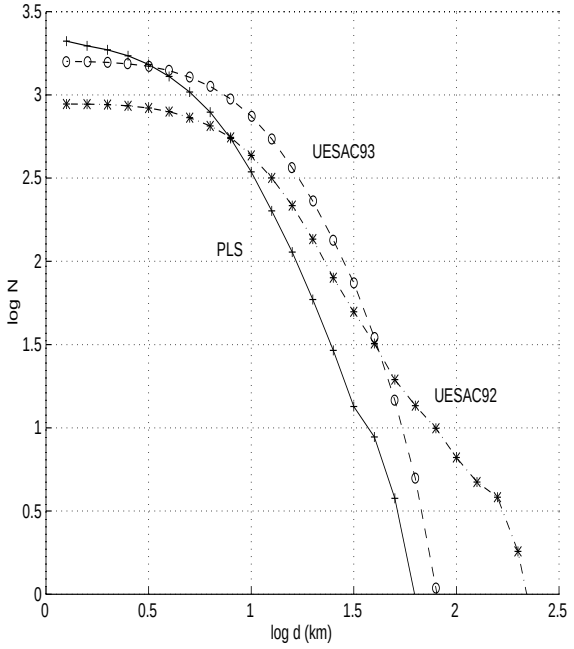

Fig. 3. The logarithm of the cumulative number of asteroids per equal (0.1) log d interval for UESAC'92, UESAC'93, and PLS.

We have made an independent investigation based on geometric albedos from the IRAS Minor Planet Survey (Tedesco et al. 1992; hereafter IRAS). We have calculated the fraction (probability) for high (p = [0.10, 1.00]) and low (p=[0, 0.10]) albedo asteroids as a function of the semimajor axis (L95). The results are given in equation 8 where $g_l(a)$ and $g_h(a)$ are the low and high albedo fractions.

$$\begin{aligned} g_l(a) &= 0.0,\ a < 1.1\ A.\,U. \\ g_l(a) &= 0.427a - 0.468,\ 1.1 \leq a < 3.4\ A.\,U. \\ g_l(a) &= 1.0,\ a \geq 3.4\ A.\,U. \\ g_h(a) &= 1.0 - g_l(a) \end{aligned} \tag{8}$$

1) The probability for the asteroid to have low ($p < 0.10$) geometric albedo is calculated using relation (8).

2) A random value, evenly distributed in the interval [0, 1] decides albedo class. If the random number is lower than the probability calculated in step 1, the low albedo class is chosen; if the random number is higher, the high albedo class is chosen.

3) The geometric albedo is randomly chosen from the corresponding normally distributed albedo function with mean value and standard deviation given in Table 6 (L95). The values in Table 6 are based on geometric albedos from IRAS. The above approach can produce erroneous albedos for individual asteroids, but the distribution for a large set of asteroids is reasonably correct. Given the geometric albedo and absolute magnitude, the formula

$$\log_{10} d = 3.122 - 0.5 \log_{10} p - 0.2H \tag{9}$$

Table 6. Mean values and standard deviations for the two geometric albedo distributions.

	$\overline{p}$	σ_p
$p_{<0.10}$	0.053	0.014
$p_{>0.10}$	0.203	0.068

was used to calculate a model-diameter d in kilometers (Bowell and Lumme 1979). The above diameter calculation was done for all UESAC and PLS asteroids with a determined orbit. Fig. 3 shows the cumulative number per equal (0.1) log d interval for UESAC'92, UESAC'93 and PLS asteroids. The linear parts of the curves can be represented by expressions of the form:

$$\log N_{1992} = 4.59 - 1.91 \log d \tag{10}$$

$$\log N_{1993} = 4.93 - 2.00 \log d \tag{11}$$

$$\log N_{PLS} = 5.39 - 2.81 \log d \tag{12}$$

The expressions are based on points in the interval $log\ d$ = [1.0, 1.5].

5. Orbital elements

The orbital elements for the new UESAC asteroids were calculated at the Minor Planet Center. When dealing with observed arcs of less than seven days, it was often necessary to make some assumption about the orbit in order to get convergence.

For previously observed asteroids, numbered and unnumbered, we have used orbital elements from EMP/MPC files. Elements for all observed numbered and un-numbered asteroids

Table 7. Number of asteroids in each orbital element category.

Survey	$T \leq 15$	$T > 15$	Multi-opp.	Total
1992	439	150	294	883
1993	834	457	299	1590

have been included, even if only one or two UESAC positions were available. We divide the elements in three categories: 1) one-opposition elements based on arc-lengths, T, $\leq$ 15 days; 2) one-opposition elements based on $T > 15$ days; 3) multi-opposition elements, including the elements for the observed numbered asteroids. The numbers of asteroids in each category are given in Table 7.

5.1. Accuracy of the orbital elements

We define the mean error for the one-opposition elements as the mean difference between the elements for the observed numbered asteroids (calculated with UESAC observations) and the elements published in EMP/MPC. Since the element accuracy is dependent on the arc-length covered by the observations we perform the error analysis separately for the element categories 1) and 2). Orbits could be calculated for 159 observed numbered asteroids based on UESAC observations with $T > 15$ days. The average differences, EMP/MPC minus survey, at the epoch 1992 March 19.0 TDT (standard epoch in the EMP and MPC versions we used) are:

$$\begin{array}{llll} \overline{|\Delta a|} & = 0.0106\ A.U. & \overline{\Delta a} & = -0.0028\ A.U. \\ \overline{|\Delta e|} & = 0.0145 & \overline{\Delta e} & = -0.0015 \\ \overline{|\Delta i|} & = 0\overset{\circ}{.}1027 & \overline{\Delta i} & = -0\overset{\circ}{.}0279 \\ \overline{|\Delta \Omega|} & = 0\overset{\circ}{.}4526 & \overline{\Delta \Omega} & = +0\overset{\circ}{.}0564 \\ \overline{|\Delta \omega|} & = 6\overset{\circ}{.}4669 & \overline{\Delta \omega} & = -1\overset{\circ}{.}1463 \\ \overline{|\Delta M|} & = 6\overset{\circ}{.}9714 & \overline{\Delta M} & = +3\overset{\circ}{.}0293 \end{array}$$

Orbits could be calculated for 124 observed numbered asteroids based on UESAC observations with time-arcs $\leq$ 15 days. In some cases the arc-lengths were too short to yield reasonable orbits; these asteroids were excluded from the error analysis. No attempt was made to obtain e-assumed orbits. The average differences, EMP/MPC minus survey, at the epoch 1992 March 19.0 TDT are:

$$\begin{array}{llll} \overline{|\Delta a|} & = 0.0638\ A.U. & \overline{\Delta a} & = -0.0226\ A.U. \\ \overline{|\Delta e|} & = 0.0689 & \overline{\Delta e} & = -0.0320 \\ \overline{|\Delta i|} & = 0\overset{\circ}{.}8805 & \overline{\Delta i} & = +0\overset{\circ}{.}2294 \\ \overline{|\Delta \Omega|} & = 2\overset{\circ}{.}5114 & \overline{\Delta \Omega} & = +0\overset{\circ}{.}0570 \\ \overline{|\Delta \omega|} & = 35\overset{\circ}{.}7418 & \overline{\Delta \omega} & = +4\overset{\circ}{.}1370 \\ \overline{|\Delta M|} & = 39\overset{\circ}{.}7839 & \overline{\Delta M} & = +1\overset{\circ}{.}4156 \end{array}$$

5.2. Statistics of semimajor axes

The distribution of the semimajor axes for the numbered asteroids show gaps at the points were the asteroid orbital period is commensurable with that of Jupiter's mean distance. This is also true for the UESAC and PLS asteroids; see Fig. 4. The distribution of the semimajor axes for the numbered asteroids does not indicate any great differences between the number of asteroids located in the inner and outer belt. It is important, however, to include only asteroids with sizes larger than a certain completeness threshold. This threshold is obviously higher in the outer belt because the larger heliocentric distances prevents observations of small objects. The thresholds cannot be very well determined since the diameter information for the numbered asteroids is limited. Accurate diameters are not needed in principle; it is more important that all diameters are determined in the same manner and that the diameter distribution is correct. A completeness threshold which is valid for UESAC and PLS asteroids was established. A conservative estimate, based on the deflection from linearity in the $log\ d - log\ N$ diagram (Fig. 3), is 15 km for UESAC and 10 km for PLS. In Fig. 6 all UESAC and PLS asteroids with model-diameters larger than two different sets of thresholds are included. This result tells us that the outer main-belt asteroids are more numerous. We can rule out the possibility that the outer main-belt asteroids are generally larger (a situation which can produce a similar effect) since the result does not change significantly with different thresholds. Also the large numbered asteroids show the same pattern. For main-belt asteroids with absolute magnitudes up to H = 11 essentially all have been found. This is shown in Fig. 5. However, the majority of the asteroids in the UESAC and PLS surveys have absolute magnitudes above H = 11. A possible explanation for the smaller number of asteroids in the inner part of the asteroid belt is that here the mechanism for transforming the orbits into planetcrossing ones is more efficient.

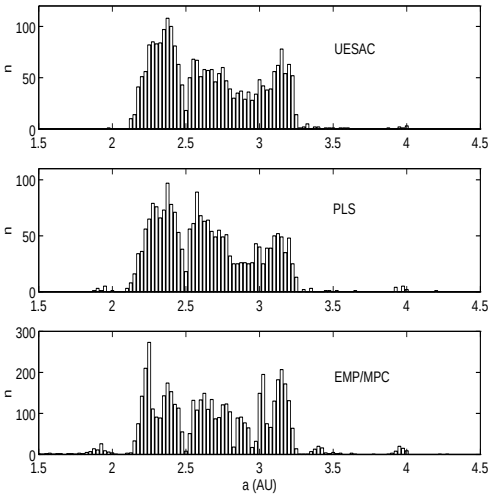

Fig. 4. Histograms of the semimajor axis for UESAC, PLS and 5297 numbered EMP/MPC asteroids.

5.3. Eccentricities and inclinations

Fig. 7 presents the eccentricities for the UESAC, PLS and 5297 numbered EMP/MPC asteroids (UPE hereafter). The PLS data seem to be slightly biased towards greater eccentricities which

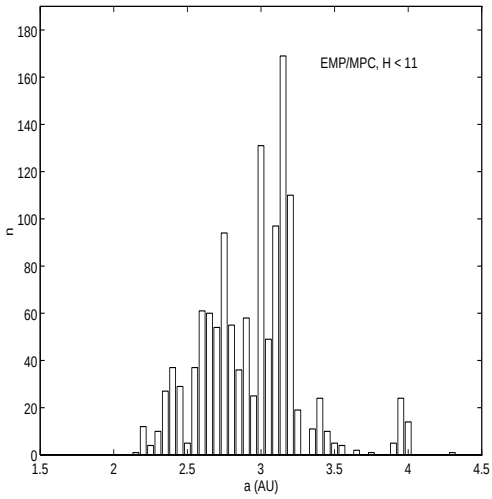

Fig. 5. Histogram of the semimajor axis for 5297 numbered EMP/MPC asteroids, $H < 11$.

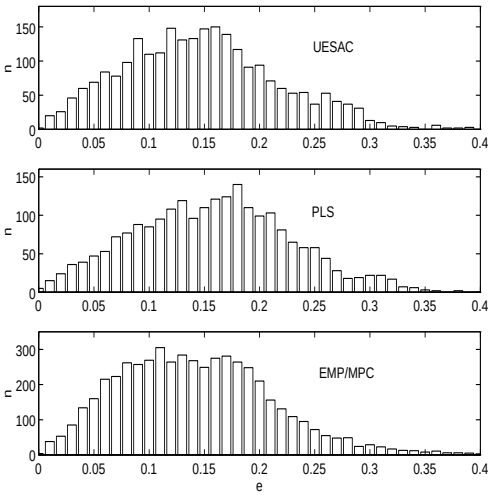

Fig. 7. Histograms of the eccentricities for UESAC, PLS and 5297 numbered EMP/MPC asteroids.

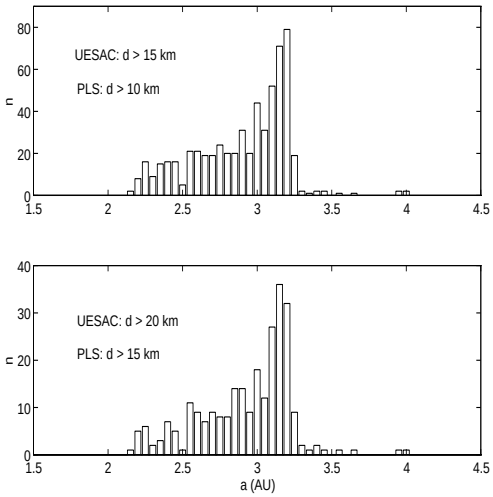

Fig. 6. Histograms of the semimajor axis for UESAC and PLS asteroids larger than different completness thresholds.

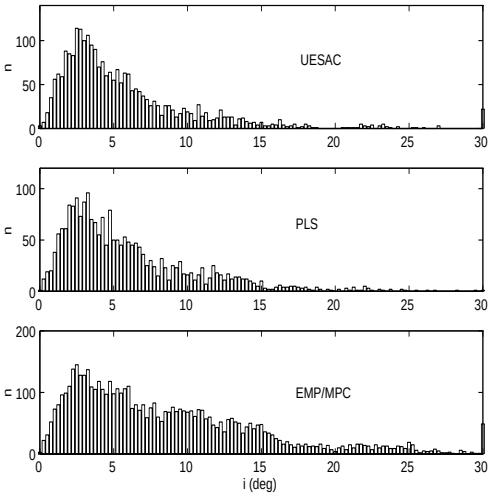

Fig. 8. Histograms of the inclinations for UESAC, PLS and 5297 numbered EMP/MPC asteroids.

may be a result of the larger fraction of PLS asteroids with longitudes of perihelion ($\omega + \Omega$) aligned with that of Jupiter. Fig. 8 presents the inclinations for UPE. The abundance of asteroids with high inclinations is lower for the UESAC and PLS asteroids. This was an expected result since both UESAC and PLS were focusing on a small region of sky close to the ecliptic.

5.4. True anomaly and longitude of the perihelion ($\omega + \Omega$)

Fig. 9 shows the true anomaly, f, at the mean epoch of the observations for UESAC and PLS. The major part of the PLS asteroids were observed close to perihelion ($f = 0°$) while the true anomalies for the UESAC asteroids have a much wider distribution. Fig. 10 displays the deviation from Jupiter's longitude of perihelion for UPE. The numbered and PLS asteroids show a clear alignment with Jupiter's perihelion; this is seen to a much lesser degree for the UESAC asteroids. In both campaigns, the ecliptic longitude of the central UESAC region was close to the direction of Jupiter's aphelion. The result is a lower abundance of asteroids aligned with Jupiter since a substantial part of the observed UESAC asteroids are close to perihelion and can thus not have their longitude of perihelia aligned with Jupiters. If we instead plot the deviation from Jupiters longitude of perihelion only for asteroids with diameters large enough to ensure that we have completeness we get the result shown in Fig. 11. Neither asteroids in PLS or UESAC show any alignment with Jupiters longitude of perihelion. For the numbered EMP/MPC asteroids larger than 50 km (adopted completness threshold for the found main-belt asteroids) the alignment can still be seen, although it is less prominent. Could the difference between the larger EMP/MPC asteroids and the UESAC and PLS asteroids larger than the completness thresholds, most of

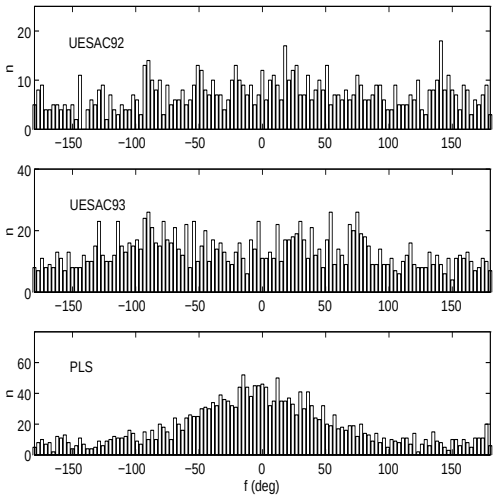

Fig. 9. True anomaly at the mean epoch of the observations for UESAC'92, UESAC'93 and PLS asteroids.

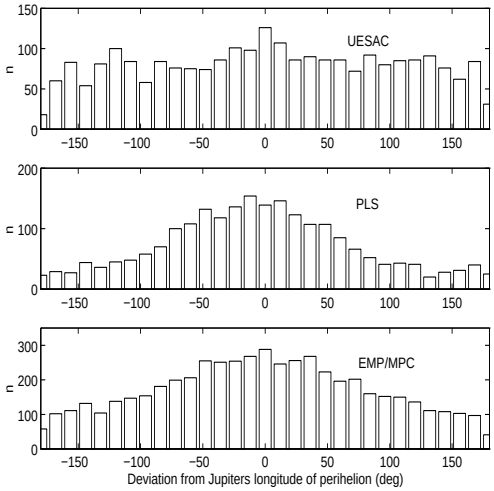

Fig. 10. Deviation from Jupiter's longitude of perihelion, $\omega + \Omega$, for UESAC, PLS and 5297 numbered EMP/MPC asteroids.

them smaller than 50 km, be a difference between large more primordial bodies and small collisional fragments ?

6. Conclusions and future work

We have compared the results in the UESAC 1992 and 1993 surveys with the PLS survey and with 5297 numbered EMP/MPC asteroids.

The statistics of the apparent and absolute magnitudes show that the slopes of the $log\ N - V$ and $log\ N - H$ curves are similar but not identical in the different surveys. This is also true for the slopes of the $log\ N - log\ d$ curves. The statistics of the three orbital elements semi-major axis, eccentricity and inclination show no major differences between UESAC, PLS and EMP/MPC asteroids. The statistics of the semi-major axis for the UESAC and PLS asteroids larger than certain completness thresholds ($d > 15\ km$ for UESAC, $d > 10\ km$ for PLS) indicate that the asteroids in the outer belt are more numerous. We show that the alignment with Jupiter's longitude of perihelion seen for the numbered EMP/MPC asteroids cannot be seen for the asteroids in UESAC and PLS larger than the above mentioned completness thresholds. The alignment with Jupiter is, however, still present for the larger EMP/MPC ($d > 50\ km$) asteroids. We raise the question if this could be a difference between large more primordial bodies and small collisional fragments; most UESAC and PLS asteroids are smaller than 50 km.

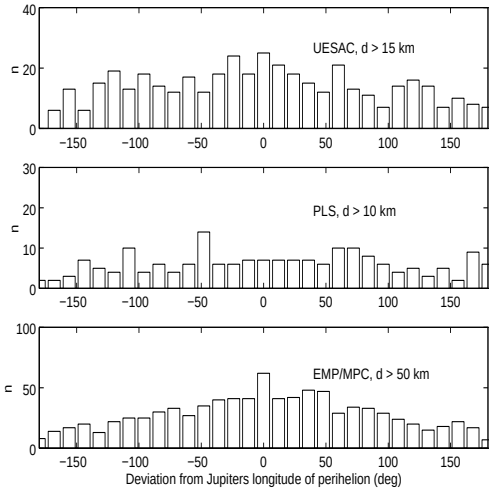

Fig. 11. Deviation from Jupiter's longitude of perihelion, $\omega + \Omega$, for UESAC, PLS and 5297 numbered EMP/MPC asteroids larger than certain completeness thresholds.

Future work should be done in understanding the reason for the statistical differences seen for asteroids with different diameters. More work should also be done to improve the orbits when more observations of the UESAC asteroids are made available.

Acknowledgements. We thank Ken Russell for obtaining the AAO films. Research supported, in part, by NorFa (Nordisk Forskerutdanningsakademi).

References

Batrakov, Y. V. (Editor-in-chief) 1993. *Efemeridy Malykh Planet 1993*. Institute for Theoretical Astronomy, St. Petersburg.

Bowell, E., Lumme, K., 1989, Colorimetry and Magnitudes, in: *Asteroids II*. eds. R. P. Binzel, T. Gehrels, M. S. Matthews, The University of Arizona.

Gradie J., Tedesco E., Compositional structure of the asteroid belt, Science, Vol. **216**, 25 June 1982.

Hernius, O., Lagerkvist, C.-I., Lindgren, M., Williams, G. V., Tancredi, G.: (1996) Astrometry of outer Jovian satellites from the Uppsala-ESO survey of asteroids and comets (UESAC). A&AS **115**, 295-296.

Ishida, K., Mikami, T. and Kosai, H., 1984. Size distribution of Asteroids, Astron. Soc. Japan **36**, 357-370.

Lagerkvist, C.-I., Hernius, O., Lindgren, M., Tancredi, G.: (1995) The Uppsala-ESO Survey of Asteroids and Comets–UESAC. In *Proc.*

from the third International Workshop on Positional Astronomy and Celestial Mechanics. (Ed. Lopez Garcia et al.), Valencia.

Lindgren, M., Tancredi, G., Lagerkvist, C.-I., Hernius, O.: 1995, Searching for Comets Encountering Jupiter: Second Campaign Observations and further Constraints on the Size of the Jupiter Family Population, A&AS, in press.

Marsden, B. G., Williams, G. V. (Editors). *Minor Planet Circulars*. Minor Planet Center, Smithsonian Astrophysical Observatory, Cambridge, U.S.A.

Röser, S. and Bastian, U., 1991, PPM star catalogue: positions and proper motions of 181731 stars north of −2.5 degrees declination for equinox and epoch; J2000.0. Astronomisches Rechen-Institut, Heidelberg.

Tancredi, G., Lindgren, M.: 1994, Searching for comets encountering Jupiter: First campaign, *Icarus* **107**, 311–321.

Tedesco, E. F., Veeder, G. J., Fowler, J. W. and Chillemi, J. R., 1992, The IRAS Minor Planet Survey Data Base, National Space Science Data Center, Greenbelt, Maryland.

van Houten, C. J., van Houten-Groenveld, I., Herget, P. and Gehrels, T., 1970: The Palomar-Leiden Survey of faint minor planets, A&AS, **2**, 339–448.

Zellner, B., and Bowell, E., 1977, Asteroid compositional types and their distributions, *Comets, Asteroids, Meteorites*, ed. A. H. Delsemme (University of Toledo Press, Toledo), p. 185.

This article was processed by the author using Springer-Verlag LaTeX A&A style file *L-AA* version 3.